



Exploiting the signal to noise ratio in multi-system predictions of summertime precipitation and maximum temperature in Europe

Juan C Acosta Navarro¹, Andrea Toreti¹

5 ¹European Commission, Joint Research Centre, Ispra, Italy

Correspondence to: Juan C Acosta Navarro (juan.acosta-navarro@ec.europa.eu)

Abstract. Droughts and heatwaves are among the most impactful climate extremes. Their co-occurrence can have devastating consequences on natural and human systems. Early information on seasonal timescales on their possible occurrence is beneficial for many stakeholders. Seasonal climate forecast has gradually become more used; but limited skill in certain regions and seasons still hinders a broader use. Here we show that a simple forecast metric from a multi-system ensemble, the signal to noise ratio, can help overcome some limitations in the boreal summer. Forecasts of maximum daily near surface air temperature and precipitation in boreal summers with high signal to noise ratio tend to coincide with observed larger deviations from the mean than years with small signal to noise ratio. The same metric also helps identify processes relevant to seasonal climate predictability. Here we show that a positive phase of a North Atlantic Sea surface dipole during boreal spring may favor the occurrence of dry and hot summers in Europe.

1 Introduction

Droughts are typically slow onset climate extreme events (Mishra and Singh, 2010), yet they can be disruptive and affect millions of people every year (Below et al., 2007; Enekel et al., 2020). Heatwaves can intensify and trigger a faster drought evolution (Bevacqua et al., 2022). Compound drought and heatwaves can have devastating consequences on socio-economic and ecological systems, and may even compromise our ability to reach the UN sustainable development goal on climate action while strongly reducing the Earth system's current natural capacity to absorb and store carbon (Yin et al., 2023). The use of seasonal climate forecasts can provide actionable information to reduce the risks and the impacts of these events on key sectors like agriculture, energy, transport, water supply (Buontempo et al., 2018; Ceglar and Toreti, 2021).

25 In the last couple of decades, climate predictions have shown important progress, they are successful in forecasting the evolution of various components of the climate system across the sub-seasonal to decadal time range (Merryfield et al., 2020; Meehl et al., 2021). Despite this progress, climate predictions still have low to moderate skill in many regions and seasons (e.g. European summer; Mishra et al. 2019); this limits their use and represents a barrier for stakeholders. A combination of



multiple forecast systems has shown overall benefits as compared with single systems and can improve forecast quality up to
30 a certain extent (Hagedorn et al., 2005; Mishra et al., 2019).

In this study we explore multi-system ensembles to test whether specific years with higher-than-normal predictability can be
detected through the local relation between skill and signal to noise ratio (SNR; section 3). We then use this proposed approach
to explore sources of summer climate predictability in Europe (Section 4).

2 Methods and data

35 The analysis is based on seasonal re-forecasts (also known as hindcasts) of mean boreal summer precipitation and 2-meter
daily maximum temperature (Tmax) for the period 1993-2016 from ECMWF SEAS5 (S5, Johnson et al., 2019), UKMO
GloSea6 (S600, MacLachlan et al., 2015), MeteoFrance (S8, Guérémy et al., 2021), CMCC (S35, Gualdi et al., 2020) and
DWD (S21, Baehr et al., 2015), available from the Copernicus C3S Climate Data Store. The observationally based datasets to
40 evaluate the re-forecasts are ERA5 (Hersbach et al., 2020) for Tmax and GPCC (Schnider et al., 2011) for precipitation. The use
of summer mean Tmax is not intended to characterize single heatwaves, but to estimate average maximum daily deviations
from the mean on a seasonal scale. In a climatological sense, more intense, more frequent or longer heatwaves than usual
generally define hot summers and hence average Tmax may be seen as a seasonal integrator of heatwave activity. Forecast
skill is evaluated with the anomaly correlation coefficient (ACC) between the ensemble mean and the observational reference.
Standardization of the anomalies of each ensemble member and the observational reference data is performed prior to the
45 analysis. This step guarantees that each member from each system has a comparable year-to-year variability to the observed
one for a particular variable. Additionally, the standardized Tmax anomalies are linearly detrended at the grid level and for
each member of the re-forecasts and in ERA5 to isolate as much as possible the impact of the long term warming. In Section
4, the Sea Surface Temperature (SST) and Geopotential Height (500 hPa, GPH500) fields are taken from ERA5 and ERSSTv5
(Huang et al., 2017), respectively.

50

In addition to the ACC, the metric computed as the product of the average multi-system ensemble mean deviation from the
long term mean and the intrinsic ensemble coherence (inverse of standard deviation) is calculated with the signal to noise ratio
for both Tmax and precipitation: $SNR = \frac{\mu_e}{\sigma_e}$, where μ_e is the multi-system ensemble mean and σ_e is the multi-system standard
deviation after standardization, computed across ensemble members for every summer (June - August) and for each gridbox.

55 25 members per system were used to have an equal contribution from each system.



3 Results

3.1 Signal to noise ratio and forecast skill

Figure 1 displays spatial maps of mean (boreal) summer Tmax ACC, time averaged SNR, and a scatter plot which shows the local relation between ACC and SNR. On average, skill values over land increase with higher SNR values. Negative values of ACC are nearly non-existent when the threshold of SNR exceeds the value of about 0.5 in the same gridbox. Statistically significant skill in Tmax is mostly confined to the tropics and sub-tropics. However, significant skill is also found in western North America, the eastern Mediterranean, central Asia and southern South America. Notable exceptions in the tropics are the Congo and parts of the Amazon rainforests. The patterns of SNR mirror those of ACC. There is a good agreement between areas of high skill (ACC) and areas with high SNR, something that is further confirmed by the local relation between ACC and SNR (Fig. 1c).

Precipitation follows a similar behavior in terms of ACC and SNR, although statistically significant skill is less widespread (Fig. 1d-f). Areas under the influence of El Nino Southern Oscillation (ENSO; Lenssen et al., 2020) appear as regions with significant ACC and high SNR. Skillful values are mostly located in the Americas, the Maritime continent and Australia. Precipitation skill and SNR in Africa and Asia are much lower, making these the regions with the largest qualitative differences between the two variables.

Based on the observed link between skill and SNR, we use the latter one as the single criterion to exclude from the re-forecasts years with very low and very high values to understand their impact on skill. When 25% of the years (6 in total) with the highest SNR (Fig. 2a) are excluded, the results overall show much lower values of ACC than when only 25% of the years with the lowest SNR are excluded (Fig. 2b). Furthermore, differences between the latter and the former result in many cases in higher values and more statistical significance than the ACC computed when only selecting years without the highest SNR (Fig. 2a,c). This result highlights the importance that these extreme SNR years can have on skill. In fact, only skill values computed when excluding the bottom 25% of SNR years (Fig. 2b) are comparable to the ones estimated when all years are used for the computation (Fig. 1a).

Interestingly, using the same criterion to select ERA5 Tmax values reveals that in general, excluding years with high ensemble SNR results in lower absolute deviations from the mean than when the low SNR years are excluded (Fig. 2d). Additionally, these differences overall coincide with regions with significant skill differences (Fig. 2c,d). This implies that years with more extreme deviations from the mean (in the observations/reanalysis) may be identified a priori by calculating the ensemble SNR of the forecast, and that forecast systems are in general more skillful when large deviations from the mean occur. A notable exception is northwestern Europe, where an opposite behavior is identified; however, it vanishes when a later initialization (June) is used.



90 Similarly, the exclusion of years with high SNR also results in lower overall precipitation skill values than the one obtained
when excluding low SNR years (Fig. 3a,b). Important skill differences appear in the Iberian Peninsula, Brazil, Australia and
Indonesia (Fig. 3c), and in most cases imply an increase from non-significant to significant skill (Fig. 3 a and b, respectively).

Contrasting with Tmax, the relation between ACC and mean absolute deviation from the mean in the observations is not
95 obvious for precipitation (Fig. 3c,d). To further investigate this behavior, we analyzed the relationship between skill differences
and the differences in absolute deviation from the mean for Tmax and precipitation, as usual using the re-forecasts that exclude
the 25% of the years with the lowest and the highest SNR, respectively. This analysis (not shown) confirms a statistically
robust relationship between skill and large deviations from mean observed precipitation, but still weaker than for Tmax.

100 Figure 4 shows a clearer relation between the impact on skill of the most extreme years in terms of SNR and the absolute Tmax
anomalies in ERA5, as compared with Figure 2. There is a good correspondence in all continents, including parts of Europe
(Fig. 4 c,d) as opposed to the results presented in Figure 2. The only difference between the two figures is that they show the
results from re-forecasts with different initialization dates. Both target the summer months (June-August), but Figure 2 shows
the results from the May initialization and Figure 4 shows the results from the June initialization. In addition, similar qualitative
105 conclusions can be made for precipitation (not shown).

3.2. Sources of climate predictability in Europe

Figure 5 shows how the ensemble SNR can also be applied to explore and understand sources of predictability and related
110 climate processes. Figure 5a displays the time series of the SNR ratio (black) of the June initialized re-forecasts and the absolute
value of the standardized ERA5 Tmax anomalies (gray) over Europe (defined in the area within 35-65N - 10W-35E, green
box in Fig. 5d). The six years with the highest Tmax SNR in Europe are 1994, 2003, 2004, 2006, 2013 and 2015 (green dots
in Fig. 5a), while the years with the lowest and the highest Tmax anomalies in Europe (after detrending) are 1993, 1996 and
2004, and 1994, 2003, and 2006, respectively (blue and red dots in Fig. 5a, respectively).

115 In terms of precipitation the largest SNR values are reached in 1994, 1997, 2003, 2006, 2011 and 2015, while the highest and
lowest observed precipitation anomalies occur in 1997, 2010 and 2011 and 1994, 1996 and 2003, respectively. Common years
with high absolute anomalies and high ensemble SNR are 1994, 2003, 2004, and 2006 for Tmax and 1994, 1997, 2003 and
2011 for precipitation. The summers of 1994 and 2003 have been documented as both dry and hot in Europe (e.g. Toreti et al.,
120 2019) and also show high ensemble SNR for both Tmax and precipitation. These years are therefore good candidates to explore
possible sources of predictability. Anomalies of 1994 and 2003 of observed summer SST and GPH500 reveal a dipole of
positive SST anomalies in the western North Atlantic and negative SST anomalies in the central/eastern North Atlantic (Fig.



5d), and a stationary Rossby wave pattern in the summer with anticyclonic anomalies in the western North Atlantic, western/central Europe and central Russia, and cyclonic anomalies in the central/eastern North Atlantic, eastern
125 Europe/western Asia and northeastern Asia.

We hypothesize that years with a strong dipole in North Atlantic SST anomalies could precondition atmospheric flow, affecting hydroclimatic summer conditions in Europe. To test this hypothesis, we created an observed spring SST index (Fig. 5c) measuring the dipole strength defined as the difference in mean SST in the western and central/eastern centers of action (green
130 boxes in Fig. 5e). Between 1982 and 2022, the years with the strongest dipole are identified before 1994 and after 2014, while years with the weakest dipole are almost exclusively found in the period 1995-2010, pointing to decadal/multi-decadal variability. A composite of summer SSTs and GPH500 (Fig. 5e), defined as the respective difference between the top 25% and the bottom 25% years based on the spring index, reveals similar patterns than those observed in 1994 and 2003 (Fig. 5d). The SST index estimated in spring is associated with persistent SST anomalies well into the summer. These long lasting SST
135 anomalies appear to force (or reinforce) a stationary Rossby wave train that induces both dry and hot summer conditions over most of Europe.

To further demonstrate the importance of this North Atlantic dipole for European summer climate, Figure 6 displays the added value of selecting each year the 60% of ensemble members that better reproduce the North Atlantic dipole index in the summer.
140 The ranking is based on the values of the squared error of the index from each member with respect to ERA5. The reduced ensemble shows a clear, consistent and statistically significant improvement of skill of summer Tmax (Fig. 6a,b) and precipitation (Fig. 6c,d) in central and northwestern Europe for re-forecasts initialized in May (Fig 5a,c) and June (Fig 5b,d) as compared to the full ensemble. These improvements are only achieved by subsampling the members based on the summer dipole index for re-forecasts initialized in May and June. When the subsampling of members is based on the May index of the
145 May initialized re-forecasts, there are no improvements of summer Tmax or precipitation skill in Europe, most likely because there is neither an improvement in the representation of the dipole in the summer (not shown).

4 Discussion

We have shown that a simple metric like the signal to noise ratio in a multi-system ensemble contains valuable information which can be used to inform in advance on possible exceptional years with large temperature and precipitation anomalies and
150 extremes.

The SNR also provides valuable information to detect potential sources of predictability. We have shown that, despite overall low skill, impactful events (i.e. anomalously dry and hot European summers) seem to be favored by a preceding dipole of high and low surface temperature anomalies in the western and central/eastern North Atlantic. These anomalies are identified in
155 spring, persist through the summer and are associated with an anomalous stationary wave pattern showing anticyclonic

conditions over most of Europe, a prime driver of hot/dry summer conditions. Note that the composite analysis also reveals anomalously warm SSTs in the North Pacific, especially marked on the eastern flank. Therefore, a remote influence of the Pacific Ocean on the North Atlantic and Europe cannot be discarded. Dunstone et al. (2019) associate precipitation anomalies in central/northern Europe with a tripole pattern of North Atlantic SSTs in spring, which has the two northernmost centers of action partially collocated with the two centers of action here identified, hence qualitatively agreeing with our findings. Nedderman et al. (2019) also show that ensemble subsampling selecting members that best reproduce a process involving North Atlantic SSTs in spring followed by a Rossby wave train in late summer largely improves temperature forecasts in central/south-western Europe. Finally, the findings presented here also agree with the ones reported by Acosta Navarro et al. (2022), which show that improved forecasts of central North Atlantic SSTs in late spring/early summer increase skill in Europe during late summer thanks to a better-simulated atmospheric circulation.

Significant skill improvements of Tmax and precipitation can be achieved in central and north-western Europe by subsampling ensemble members that better follow the evolution of the observed North Atlantic dipole temperature index during summer. Selecting members of the re-forecasts initialized in May that better agree with the observed dipole index in May, results in no clear improvement in the summertime dipole index or in the European climate. This points to the need for further efforts and analyses to understand this unexpected behavior. The proposed detection method based on ensemble SNR and North Atlantic SST pattern found here is nonetheless useful to explore sources of atmospheric predictability for summer forecasts in Europe and could likely be applied to other regions and seasons.

References

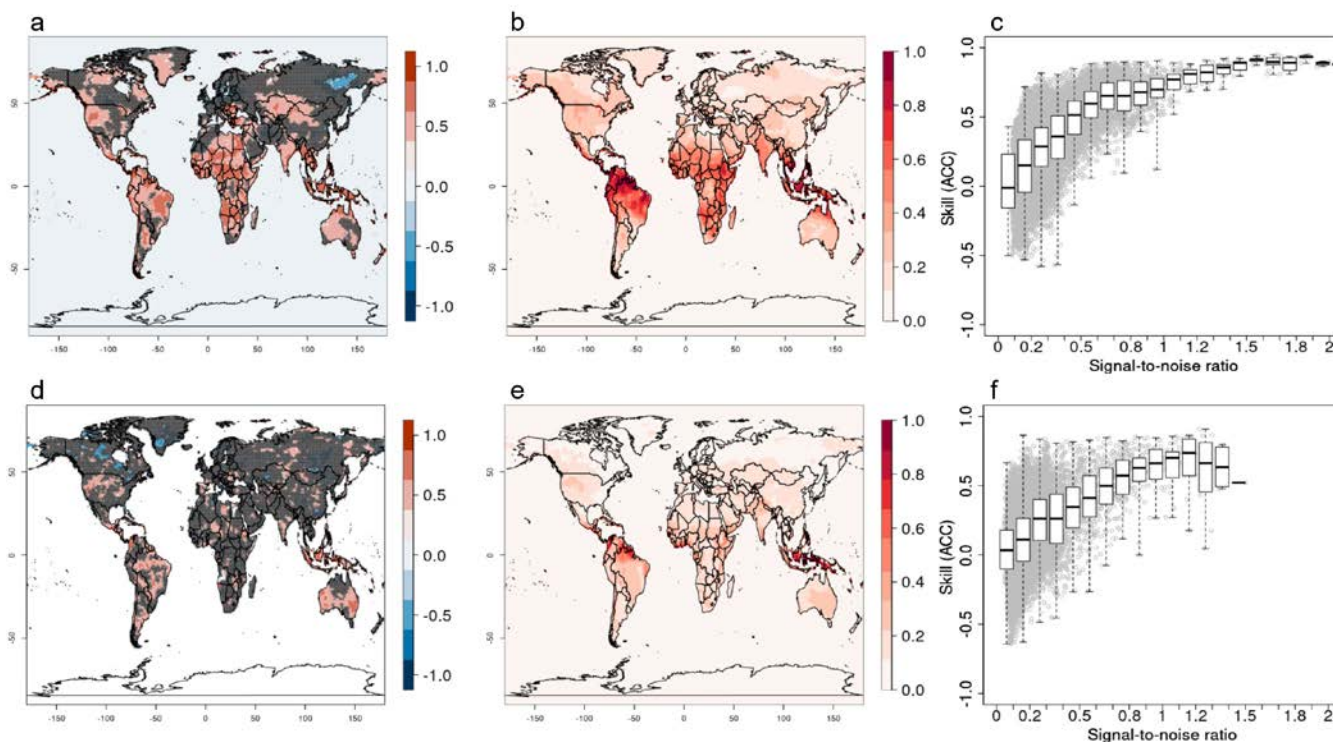
- Acosta Navarro, J. C., García-Serrano, J., Lapin, V., and Ortega, P.: Added value of assimilating springtime Arctic sea ice concentration in summer-fall climate predictions. *Environmental Research Letters*, 17(6), 064008, doi: 10.1088/1748-9326/ac6c9b, 2022.
- Baehr, J., Fröhlich, K., Botzet, M. et al.: The prediction of surface temperature in the new seasonal prediction system based on the MPI-ESM coupled climate model. *Clim Dyn* 44, 2723–2735. doi: 10.1007/s00382-014-2399-7, 2015
- Below, R., Grover-Kopec, E., and Dilley, M.: Documenting drought-related disasters: A global reassessment. *The Journal of Environment & Development*, 16(3), 328-344. doi: 10.1177/1070496507306222, 2007.
- Bevacqua, E., Zappa, G., Lehner, F., and Zscheischler, J.: Precipitation trends determine future occurrences of compound hot-dry events. *Nature Climate Change*, 12(4), 350-355. doi: 10.1038/s41558-022-01309-5, 2022.



- 190 Buontempo, C., Hanlon, H. M., Soares, M. B., et al.: What have we learnt from EUPORIAS climate service prototypes? *Climate Services*, 9, 21-32. doi: 10.1016/j.cliser.2017.06.003, 2018.
- 195 Dunstone, N., Smith, D., Scaife, A., et al.: Skilful seasonal predictions of summer European rainfall. *Geophysical Research Letters*, 45(7), 3246-3254. doi: 10.1002/2017GL076337, 2018.
- Ceglar, A., and Toreti, A.: Seasonal climate forecast can inform the European agricultural sector well in advance of harvesting. *npj Clim Atmos Sci* **4**, 42. doi: 10.1038/s41612-021-00198-3, 2021.
- Enenkel, M., Brown, M.E., Vogt, J.V. et al.: Why predict climate hazards if we need to understand impacts? Putting humans back into the drought equation. *Climatic Change* **162**, 1161–1176. doi: 10.1007/s10584-020-02878-0, 2020.
- 200 Gualdi, S., A. Sanna, A. Borrelli, A., et al.: The new CMCC Operational Seasonal Prediction System SPS3.5. *Centro Euro-Mediterraneo sui Cambiamenti Climatici. CMCC Tech. Note RP0288*, 26pp. doi: 10.25424/CMCC/SPS3.5, 2020.
- Guérémy, J. F., Dubois, C., Viel, C., et al.: Assessment of Météo-France current seasonal forecasting system S7 and outlook on the upcoming S8. In *EGU General Assembly Conference Abstracts* (pp. EGU21-10185), 2021.
- 205 Hagedorn, R., Doblas-Reyes, F. J., and Palmer, T. N.: The rationale behind the success of multi-model ensembles in seasonal forecasting—I. Basic concept. *Tellus A: Dynamic Meteorology and Oceanography*, 57(3), 219-233. doi: 10.3402/tellusa.v57i3.14657, 2004.
- 210 Hersbach, H., Bell, B., Berrisford, P., Hirahara, S., et al.: The ERA5 global reanalysis. *Quarterly Journal of the Royal Meteorological Society*, 146(730), 1999-2049. Doi: 10.1002/qj.3803, 2020.
- Huang, B., Thorne, P. W., Banzon, V. F., et al.: NOAA extended reconstructed sea surface temperature (ERSST), version 5. *NOAA National Centers for Environmental Information*, 30, 8179-8205. Doi: 10.1175/JCLI-D-16-0836.1, 2017.
- 215 Johnson, S. J., Stockdale, T. N., Ferranti, L., et al.: SEAS5: the new ECMWF seasonal forecast system. *Geoscientific Model Development*, 12(3), 1087-1117. Doi: 10.5194/gmd-12-1087-2019, 2019.
- 220 Lenssen, N. J., Goddard, L., and Mason, S.: Seasonal forecast skill of ENSO teleconnection maps. *Weather and Forecasting*, 35(6), 2387-2406. Doi: 10.1175/WAF-D-19-0235.1, 2020.

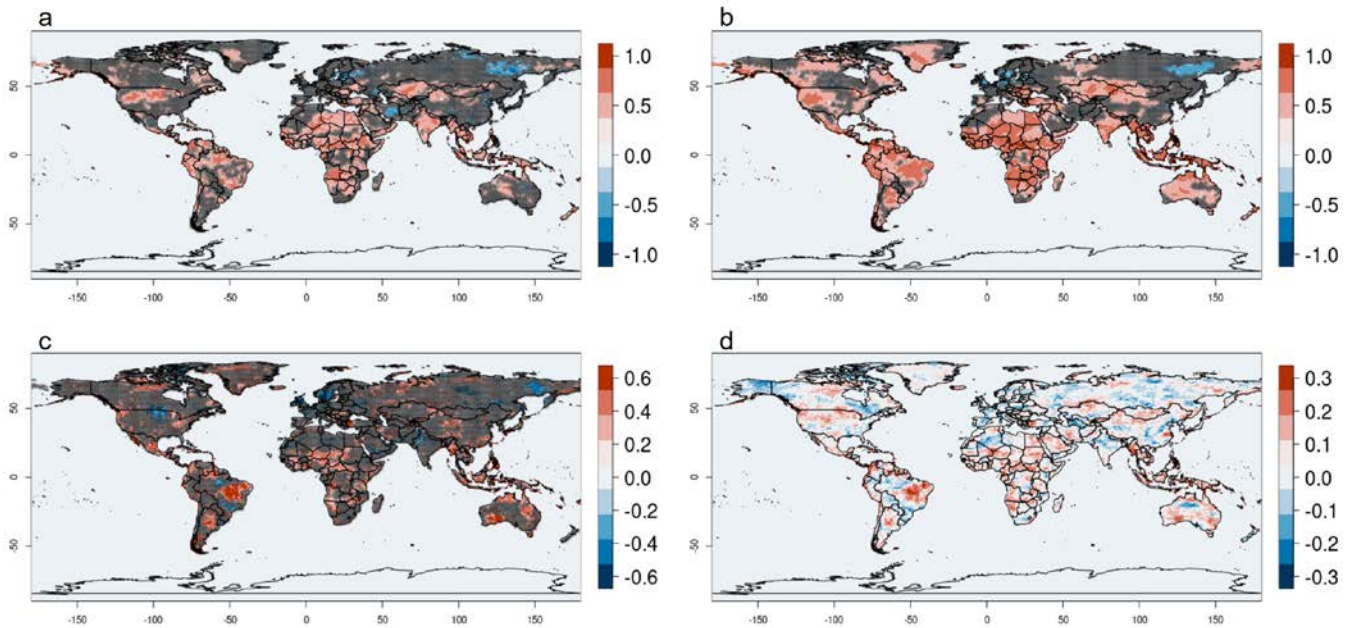


- MacLachlan, C., Arribas, A., Peterson, K. A., et al: Global Seasonal forecast system version 5 (GloSea5): A high-resolution seasonal forecast system. *Quarterly Journal of the Royal Meteorological Society*, 141(689), 1072-1084. doi.org/10.1002/qj.2396, 2015.
- 225
- Meehl, G. A., Richter, J. H., Teng, H., et al.: Initialized Earth System prediction from subseasonal to decadal timescales. *Nature Reviews Earth & Environment*, 2(5), 340-357. Doi: 10.1038/s43017-021-00155-x, 2021.
- Merryfield, W. J., Baehr, J., Batté, L., et al.: Current and emerging developments in subseasonal to decadal prediction. *Bulletin of the American Meteorological Society*, 101(6), E869-E896. doi: 10.1175/BAMS-D-19-0037.1, 2020.
- 230
- Mishra, A. K., and Singh, V. P.: A review of drought concepts. *Journal of hydrology*, 391(1-2), 202-216. doi: 10.1016/j.jhydrol.2010.07.012, 2010.
- 235
- Mishra, N., Prodhomme, C., and Guemas, V.: Multi-model skill assessment of seasonal temperature and precipitation forecasts over Europe. *Climate Dynamics*, 52(7), 4207-4225. , 2019.
- Neddermann, N. C., Müller, W. A., Dobrynin, M., et al.: Seasonal predictability of European summer climate re-assessed. *Climate Dynamics*, 53(5), 3039-3056. doi: 10.1007/s00382-019-04678-4, 2019.
- 240
- Schnider, U., Becker, A., Finger, P., et al.: GPCP Full Data Reanalysis Version 6.0 at 1.0°: Monthly Land-Surface Precipitation from Rain-Gauges built on GTS-based and Historic Data. Doi: 10.5676/DWD_GPCC/FD_M_V6_100, 2011.
- Toreti, A., Belward, A., Perez-Dominguez, I., et al.: The exceptional 2018 European water seesaw calls for action on adaptation. *Earth's Future*, 7(6), 652-663. doi: 10.1029/2019EF001170, 2019.
- 245
- Yin, J., Gentine, P., Slater, L., et al.: Future socio-ecosystem productivity threatened by compound drought–heatwave events. *Nature Sustainability*, 1-14. Doi; 10.1038/s41893-022-01024-1, 2023.



250

Figure 1: June-August Skill (ACC), time averaged SNR and scatterplots of local relation between ACC and SNR for Tmax (a-c) and precipitation (d-f). Each gray dot in (c,f) represents the values of ACC and SNR at each gridbox. Gray dots in (a,d) indicate statistically non-significant values with a 90% confidence based on a t-test. The re-forecasts are initialized every May.



255

Figure 2: Skill (ACC) of Tmax predictions excluding 25% of the years with highest (a) and lowest (b) local SNR. (c) Difference between (a) and (b). (d) Difference in the time-averaged absolute deviation from the mean in ERA5 Tmax, excluding years having 25% of the lowest and highest local SNR, respectively. Gray dots in (a-c) indicate statistically non-significant values with a 90% confidence based on a t-test. The re-forecasts are initialized every May.

260

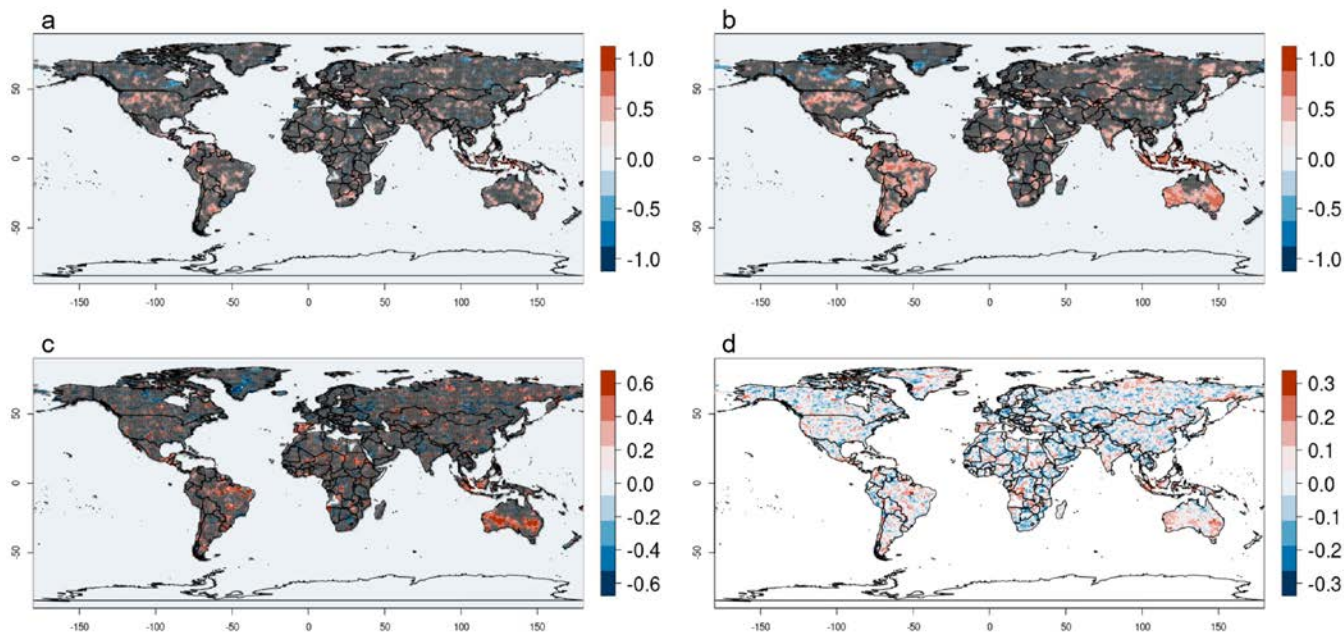


Figure 3: Same as Figure 2, but for precipitation.

265

270

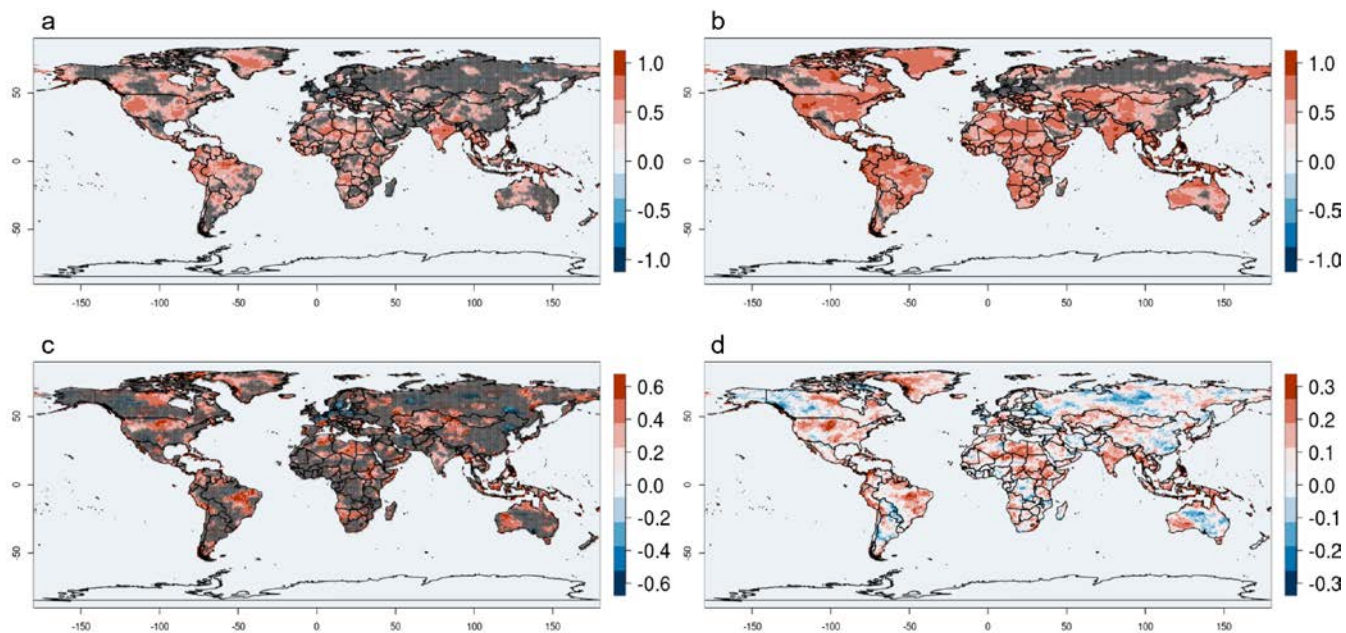


Figure 4: Same as Figure 2, but for the re-forecasts initialized in June.

275

280

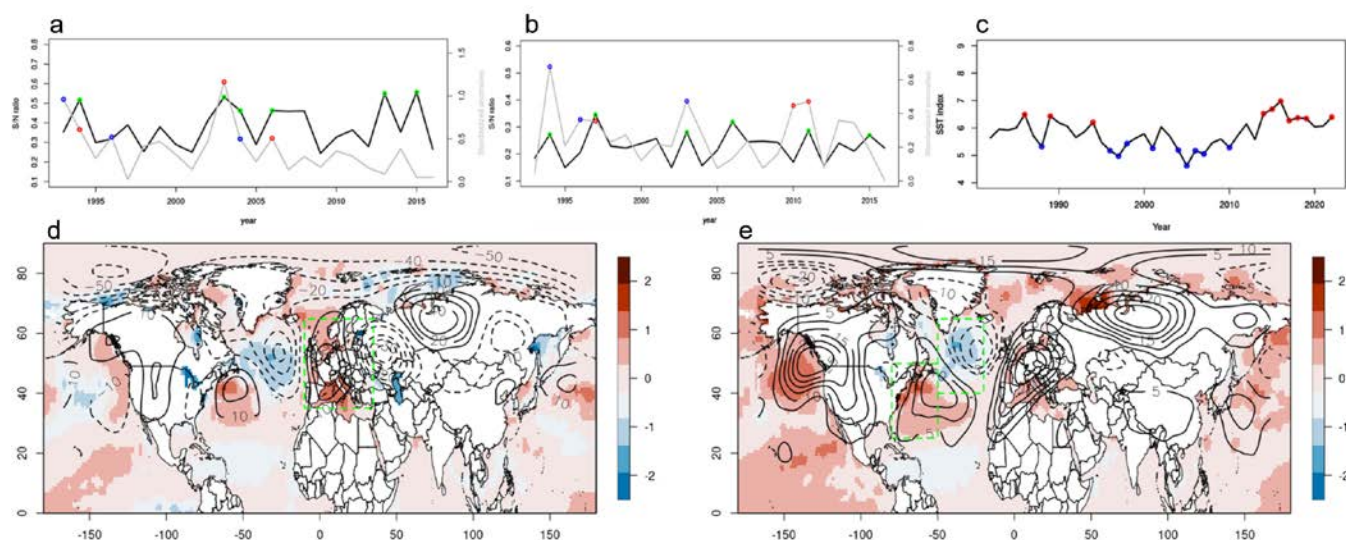


Figure 5: (a) Time series of mean spatial SNR (black line) in the re-forecasts and absolute deviation from mean (gray) for Tmax over Europe in ERA5 (green box in panel d). Blue and red dots in (a) show the top three coldest and hottest summers in Europe (after detrending), while green dots indicate the top six years in terms of Tmax SNR. (b) The same as (a) but for precipitation. Blue and red dots in (b) show the three driest and wettest summers in Europe, while green dots indicate the top six years in terms of precipitation SNR. The re-forecasts used in (a-b) are from the June initialization. (c) Time series of the index estimated as the difference between the western and central/eastern North Atlantic SST in spring (March-May). Blue and red dots indicate the 25% lowest and highest values, respectively. (d) Mean summer anomalies of SST and GPH500 for the years 1994 and 2003. Composites of summer SSTs and GPH500 for years with high minus low March-May SST index in the period 1982-2022.

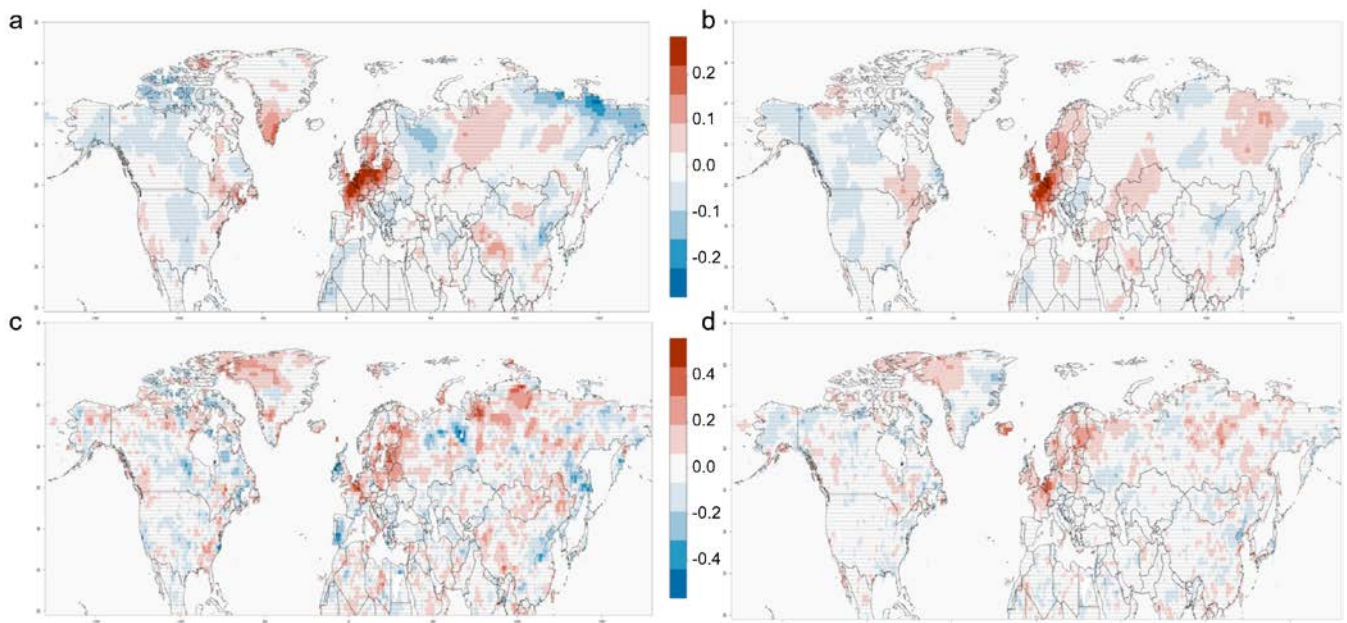
285

290

295

300

305



310 **Figure 6: Skill difference (ACC) between a selection of 60% of the members with the best JJA SST index score (lowest RMSE) and the full ensemble for summer (a) Tmax in forecasts initialized in May, (b) Tmax in forecasts initialized in June, (c) precipitation in forecasts initialized in May and (d) precipitation in forecasts initialized in June. Gray dots indicate statistically non-significant values with a 90% confidence based on a t-test.**